



## All-optical magnetization recording by tailoring optical excitation parameters

Daniel Steil,<sup>\*</sup> Sabine Alebrand, Alexander Hassdenteufel, Mirko Cinchetti,<sup>†</sup> and Martin Aeschlimann  
*Department of Physics and Research Center OPTIMAS, University of Kaiserslautern, D-67653 Kaiserslautern, Germany*

(Received 13 July 2011; revised manuscript received 24 October 2011; published 13 December 2011)

We investigate the dependency of all-optical magnetization switching on the properties of the exciting laser pulse by specifically tailoring all accessible laser parameters—pulse duration, wavelength, chirp, and bandwidth—over a wide range. Our results show that all-optical switching can be achieved with picosecond instead of femtosecond laser sources of various wavelengths, which considerably relaxes technological feasibility of this technique. The most striking implication is that, in contrast to all current knowledge, a strong photoinduced nonequilibrium in the electronic system is not necessary to achieve magnetization switching with light.

DOI: [10.1103/PhysRevB.84.224408](https://doi.org/10.1103/PhysRevB.84.224408)

PACS number(s): 75.60.Jk, 75.78.-n, 75.40.Gb, 85.70.Li

### I. INTRODUCTION

It has been recently shown that the magnetization state of ferrimagnetic rare-earth transition-metal alloys can be switched deterministically by means of circularly polarized femtosecond laser pulses without an applied magnetic field.<sup>1</sup> Depending on the helicity of light, domains with opposite magnetization were written in an out-of-plane magnetized sample with carefully chosen laser parameters. Moreover, it was possible to show by means of single shot time-resolved Faraday imaging that this change occurs in a few tens of picoseconds using laser pulses with 40-fs temporal width.<sup>2</sup> This is about two orders of magnitude faster than anything feasible without using relativistic electron sources.<sup>3</sup> Up to date, a wide variety of different experimental observations and processes connected to all-optical manipulation of magnetization have been reported.<sup>4–10</sup>

A phenomenological description of all-optical magnetization reversal was introduced by Vahaplar and co-workers.<sup>2</sup> They assumed that ultrashort laser pulses induce magnetization switching by acting on the sample in a twofold way: First, a strong nonequilibrium, whose necessity was previously postulated also in Ref. 1, is generated in the electronic system. Second, the laser pulse acts as an effective magnetic-field pulse ( $H_{\text{eff}}$ ) of several T of magnitude in the material. The origin of  $H_{\text{eff}}$  was speculated to be the inverse Faraday effect (IFE), whose existence has been already demonstrated in dielectrics.<sup>5</sup>

Although the model of Vahaplar *et al.* can describe the experimental findings, it raises one fundamental question regarding the microscopic origin of  $H_{\text{eff}}$ . In fact, magnetization reversal takes generally much longer than the laser field is interacting with the sample. As a consequence, the effective magnetic field  $H_{\text{eff}}$  assumed in theory persists for longer times than the laser field is present in the material. So how is the information about the light helicity (giving rise to the effective magnetic field) “stored” inside the medium after the laser pulse is off? This is extremely puzzling, since the typical dephasing time of an electron-hole pair generated in the material by interaction with the laser is only a few femtoseconds.<sup>11</sup>

As both  $H_{\text{eff}}$  and the strong nonequilibrium in the electronic system are generated by the light field, a variation of the laser properties should consequently influence the switching behavior. Therefore the most straightforward way to find information about the microscopic origin of  $H_{\text{eff}}$  is to systematically change the parameters of the exciting laser and to evaluate

the influence on magnetization switching. This is the strategy followed in this paper.

We have studied the influence of the pulse properties on the switching behavior of the ferrimagnetic alloy GdFeCo. The main idea of our experiments is schematically depicted in Fig. 1. We have manipulated the optical switching field by (i) introducing a positive or negative chirp; (ii) tuning the pulse length within three orders of magnitude, from 40 fs to 10 ps; (iii) changing the wavelength in the visible region (400–800 nm); and (iv) decreasing the bandwidth from 40 to 0.063 nm (78 meV to 275  $\mu\text{eV}$ ). We measured how such modifications affect the threshold laser fluence needed for magnetization reversal.

Varying the pulse duration allows us to study if a strong nonequilibrium in the electronic system is a necessary condition to achieve switching. Moreover, the validity and limitations of the IFE picture<sup>2</sup> in terms of the all-optical switching can be tested, since a variation of the pulse duration for constant intensity should lead to a change in the strength of  $H_{\text{eff}}$ , in turn affecting the switching threshold. Furthermore, models or concepts introduced to describe the microscopic origin of the IFE can be tested: Changing the wavelength allows testing the predictions made by Hertel<sup>12</sup> on the wavelength dependence of the IFE in metals. Using a microscopic model for the IFE, Hertel found a  $\omega^{-3}$  dependence of the magnetization generated by the IFE. More generally, measuring the wavelength dependency allows us to ascertain whether or not a resonant excitation might be responsible for the observed effects. Changing the chirp and the bandwidth of the laser allows us to test whether the concept of *spin-flip stimulated Raman scattering* (SF-SRS),<sup>13</sup> previously used as a microscopic model of the inverse Faraday effect in the context of laser induced magnetization dynamics in dielectrics, may be also a suitable description of all-optical-switching in GdFeCo, as it was speculated by Stanciu *et al.*<sup>1</sup>

We find that the phenomenological concept of an induced magnetic field  $H_{\text{eff}}$  fits our experimental results, while its microscopic origin still remains unclear. In particular, we show that it cannot be explained in terms of an inverse Faraday effect. Additionally our results indicate that the microscopic origin of  $H_{\text{eff}}$  is not spin-flip stimulated Raman scattering. The microscopic process seems only to depend on the number of photons and it is not a resonant one. Finally, we demonstrate that a strong nonequilibrium in the electronic system is not necessary to achieve all-optical switching.

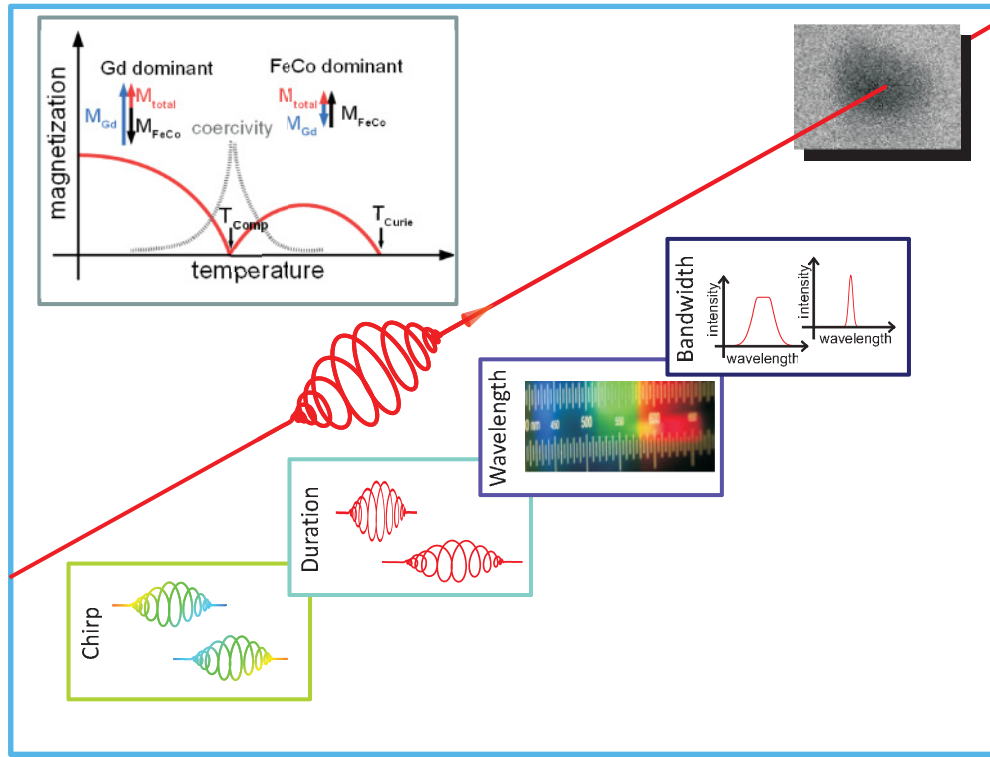


FIG. 1. (Color online) Concept of the experiments. A circularly polarized femtosecond laser pulse (red) is used to switch the magnetization of a GdFeCo sample. The switching is monitored by a Faraday imaging setup, delivering images where black and white areas correspond respectively to magnetic domains with opposite orientation (perpendicular to the sample plane). To gain information about the fundamental microscopic mechanisms underlying all-optical switching, we have tailored the represented laser parameters: chirp, pulse duration, wavelength, and bandwidth. The sample system used was  $\text{Gd}_{26}\text{Fe}_{64.7}\text{Co}_{9.3}$  (Gd26), with a compensation point of  $T_{\text{comp}} = 380$  K. The inset shows the  $M(T)$  curve for a typical ferrimagnetic system, as investigated in this paper.

## II. METHODS

The measurements were performed at room temperature on the rare-earth transition-metal alloy  $\text{Gd}_{26}\text{Fe}_{64.7}\text{Co}_{9.3}$  (short Gd26), an amorphous and ferrimagnetic alloy with out-of-plane anisotropy and compensation temperature of 380 K. The sample is a multilayer sandwich with the structure glass/AlTi (10 nm)/SiN (5 nm)/RE-TM (20 nm)/SiN (60 nm). It was provided by the group of A. Itoh, like the samples investigated in Ref. 2.

Shortly, the measurements have been performed as follows: The samples were exposed for a short time to the circularly polarized light of a fs amplifier, manipulated as discussed in detail in Secs. II A and II B below to affect chirp, pulse length, and central wavelength. The same experiment was repeated using a picosecond laser system to clearly disentangle the possible effects of pulse width and chirp on the switching and to gain additional information about the relevance of the bandwidth. Magnetic contrast was achieved using a Faraday imaging setup, described in Sec. II A. Depending on whether magnetization switching was obtained after laser exposure, the laser intensity was either increased or decreased until the minimum laser fluence leading to a magnetization switching was determined. This quantity is our physical observable and is called *threshold fluence* ( $F_{\text{min}}$ ). The measuring procedure was repeated for both sample magnetization directions and laser pulse helicities, to exclude the possibility of a helicity-independent thermal writing event.<sup>1</sup>

### A. Experimental setup and measurement procedure

Experiments have been performed using a Faraday imaging setup, where the magnetic contrast was achieved using a polarizer-analyzer combination, a zoom lens, a charge-coupled device camera, and a white light source. The sample is placed between the polarizer and the analyzer. Several different laser systems have been used to perform the experiments described in Sec. III. The experiments on chirp/pulse duration dependence using a phase pulse shaper or the amplifier compressor have been performed using a 780-nm 5–20-kHz fs amplifier system running at 5 kHz with a pulse duration of at minimum 40 fs at the sample position (the amplifier itself is capable of delivering sub-30-fs pulses) and a maximum pulse energy of 1.7 mJ/pulse. The spectral full width at half maximum (FWHM) at the sample position is  $\approx 40$  nm ( $\approx 78$  meV) for measurements using the compressor and  $\approx 32.5$  nm ( $\approx 65$  meV) for measurements using the shaper. For the nonlinear optical parametric amplifier (NOPA) measurements a 1-kHz amplifier system with 777-nm central wavelength, a spectral FWHM of  $\approx 9$  nm ( $\approx 18.5$  meV), and a pulse duration of 170 fs was used. Note that the frequency-converted NOPA pulses are generally shorter than the 170-fs fundamental pulses, at around 80 fs, due to the fact that a supercontinuum is used. To achieve longer pulse durations and much smaller bandwidths of the laser pulses a picosecond laser system with variable repetition rates between 1 Hz and 500 kHz was used. The wavelength of the system was 532 nm and

the spectral FWHM was 0.063 nm ( $\approx 275 \mu\text{eV}$ ). Pulse durations varied slightly with repetition rate from approximately 9–13 ps.

Depending on the experiment the fluence incident on the sample is tunable by both a combination of half wave plate and polarizer and/or a indexed gray filter wheel with optical density (OD) steps of 0.1 from OD 0.1 up to OD 3.0. The required helicity was obtained using a zero-order quarter wave plate for 800 nm or for the case of the NOPA/ps-laser measurements using an additional achromatic quarter wave plate for 460–680 nm, respectively a zero-order quarter wave plate for 390 nm. All data were recorded at ambient temperature.

To determine  $F_{\min}$  we applied the following measuring routine: First the sample was homogeneously magnetized in one easy axis orientation with a magnet, then the sample was exposed to the beam to write stripes. If writing was obtained, the sample was remagnetized in the same direction and afterward it was exposed to light of the opposite helicity. If writing was only possible for the proper helicity all-optical writing was achieved. The procedure was then repeated for the other magnetization direction, to double check data. For the experiments with the amplifier compressor and for single shot measurements single dots were additionally recorded with the same procedure as above, yielding no significant differences to the stripe method. For experiments with the NOPA only stripes of reversed magnetization were recorded by sweeping the beam over the sample and the fluence was reduced until reversal of magnetization was only observed for one helicity. This was necessary to minimize the error arising from the intensity fluctuation of the NOPA pulses.

### B. Tailoring of the laser pulses

The duration of the pulses was manipulated with a programmable liquid-crystal display all-reflective pulse shaper (manipulating the pulse phase). For a general overview about pulse shaping techniques we refer to Ref. 14. The pulse duration was additionally manipulated by changing the grating separation in the pulse compressor of the amplifier (for details on chirped pulse amplifiers, cf. Ref. 15). In both cases, frequency dispersion was introduced on the pulse, meaning that different frequencies in the broadband femtosecond pulse arrive at different times at the sample. This pulse broadening is dominated by the second-order dispersion term here, therefore mainly the so-called *group velocity dispersion* or GVD of the pulse was manipulated. The GVD describes the change in the envelope of the pulse due to the wavelength dependence of the group velocity in a medium:  $\frac{dv_g}{d\lambda} = \frac{\omega^2 v_g^2}{2\pi c} \frac{d^2k}{d\omega^2}$ , cf. Ref. 16. To measure the pulse duration, a mirror on a flip mount near the sample, which deflects the beam into an autocorrelator, was utilized. It was possible to achieve negative or positive pulse chirps with this setup depending on the shaper settings or the distance of the compressor gratings.<sup>17</sup>

### C. Calculations with the 2TM

For the calculation of the electron ( $e$ ) and lattice ( $l$ ) temperatures after excitation with laser pulses of variable pulse duration we used the standard two temperature model (2TM).<sup>18</sup>

The corresponding differential equations read as follows:

$$\frac{dT_e}{dt} = \frac{g_{el}(T_l - T_e) + P}{c_e}, \quad (1)$$

$$\frac{dT_l}{dt} = \frac{g_{el}(T_e - T_l)}{c_l}. \quad (2)$$

The source term  $P$  describes the laser excitation and is assumed to have a Gaussian shape with a total power and pulse duration according to the experimental values. For the electron-lattice coupling constant ( $g_{el}$ ) we utilized the same value as in Ref. 2, namely  $g_{el} = 1.7 \times 10^{18} \text{ J/K s}$ . The heat capacity of the lattice was assumed to be  $c_l = 3 \times 10^6 \text{ J/(K m}^3\text{)}$ , which also corresponds to the value used by the authors of the above-mentioned reference. The heat capacity of the electronic system was considered temperature dependent:  $c_e = \gamma T_e$  with  $\gamma = 700 \text{ J/(K}^2 \text{ m}^3\text{)}$ .

## III. EXPERIMENTAL RESULTS

Let us start by considering the influence of pulse duration and chirp on the switching. We used two independent strategies to change the pulse duration, as described in the Methods section: changing the group velocity dispersion (GVD) by using a pulse shaper or by making use of the amplifier compressor. Both methods result in a concomitant change of the pulse chirp together with the pulse duration. Figure 2 depicts the values of  $F_{\min}$  as a function of the pulse duration obtained in the experiments performed with the pulse shaper. The plot is divided into regions of positively (right half) and negatively (left half) chirped pulses by the dotted vertical line.

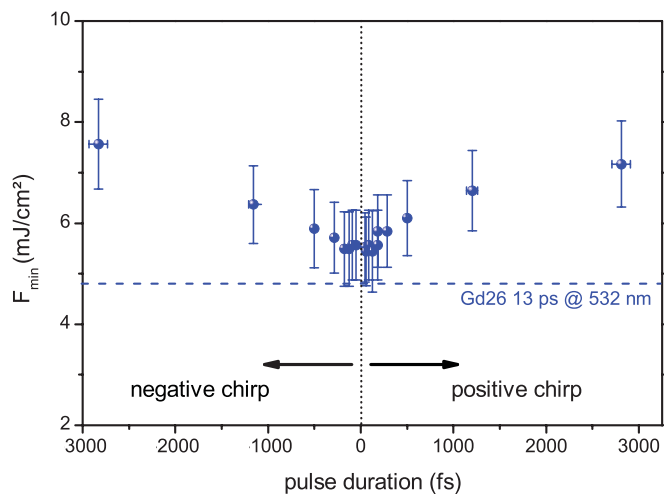


FIG. 2. (Color online) Dependence of the threshold fluence  $F_{\min}$  on the temporal duration of laser pulses with central wavelength of 780 nm. The pulse duration was manipulated by changing the GVD from approximately  $-27\,000$  to  $27\,000 \text{ fs}^2$ . Accordingly, the plot is divided into regions of positive and negative chirp by the vertical dotted line. The horizontal dashed line shows the value of  $F_{\min}$  for unchirped laser pulses with temporal width of 13 ps, central wavelength of 532 nm, and repetition rate of 5 kHz. Error bars on the y axis are calculated by error propagation including the error given by the uncertainty of the laser spot size determination (10% of the determined spot size) and by the laser power fluctuations. Error bars on the x axis are given by the fluctuations of the laser autocorrelation.

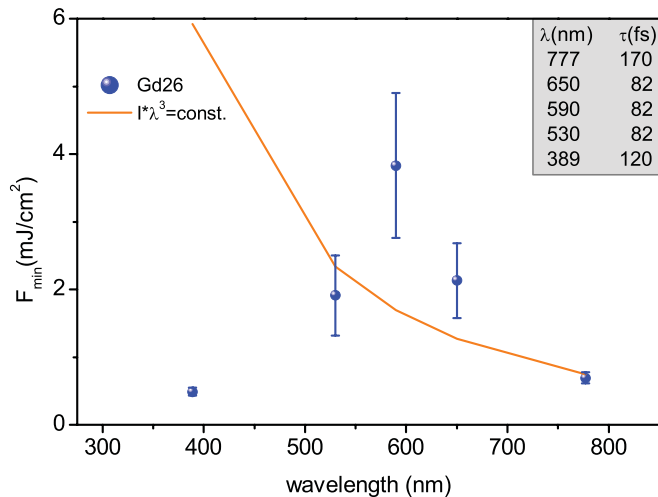


FIG. 3. (Color online) Dependence of the threshold fluence  $F_{\min}$  on the central wavelength of the exciting laser pulse. Central wavelengths and corresponding pulse widths are given in the inset. The spectra of the pulses can be found in the Supplemental Material.<sup>19</sup> Error bars are calculated as in Fig. 2, but assuming an error of 25% of the determined spot size to account for the larger inhomogeneities of the spots created by the NOPA. The solid line represents the expected wavelength dependency of  $F_{\min}$  according to the theoretical calculations in Ref. 12.

Pulse durations range from approximately 2.8 ps for negative chirp to up to 2.8 ps for positive chirp, equivalent to a huge variation in GVD from approximately  $-27\,000$  to  $27\,000$  fs<sup>2</sup>. We observe a slight increase of  $F_{\min}$  for increasing pulse length and for both signs of the chirp. The maximal increase is approximately a factor of 1.4. Remarkably, the changes in  $F_{\min}$  are by a factor of  $\approx 40$  smaller than the changes in pulse duration. This means that, independent of the pulse duration, approximately the same number of photons is needed to obtain magnetization switching. The results of the measurements performed utilizing the amplifiers internal pulse compressor show similar behavior and can be found in the Supplemental Material.<sup>19</sup>

As a second step, we changed the spectral properties of a different amplifier system with the help of a NOPA and by second harmonic generation. We chose five different central wavelengths between 389 and 777 nm (for spectra cf. Supplemental Material<sup>19</sup>). Figure 3 shows the values of  $F_{\min}$  as a function of the used wavelengths, given in the inset together with the corresponding pulse duration. Remarkably, also in this experiment all-optical switching could be achieved for all laser parameters. A trustworthy evaluation of the incident fluence needed to switch the magnetization is difficult, due to the strongly changing non-Gaussian mode shape for the different wavelengths generated in the NOPA. Therefore the observed maximum around 600 nm has to be taken with extreme care. Nevertheless, the data points for 389 and 777 nm can be compared quantitatively (because they have not been generated by the NOPA) and show approximately the same value of  $F_{\min}$ . In all cases the energy of the pulses was in the 0.4–1.0- $\mu$ J range, thus no large deviations were observed at least in incident energy.

As a third and final step, we performed an experiment using a laser source with 532 nm central wavelength, which (i) emitted much longer pulses of about 13 ps width and (ii) had a tremendously smaller spectral bandwidth of only about 0.063 nm or approximately 66.5 GHz, a factor 100–600 smaller than the bandwidths utilized in the previous experiments. The measurements were performed in a single-shot configuration and additionally in a multishot configuration with 5-kHz repetition rate. In both cases optomagnetic writing was achieved. In particular, the single shot switching threshold  $F_{\min}$  was estimated to be approximately 5.7 mJ/cm<sup>2</sup>, while the 5-kHz switching threshold  $F_{\min}$  was estimated to be slightly lower at approximately 4.8 mJ/cm<sup>2</sup>. The latter value is plotted in Fig. 2 with a dashed horizontal line. Clearly, this value is very similar to the other data plotted in Fig. 2. Again the fluences are not fully quantitatively comparable, as the mode shapes of all these lasers are different.

#### IV. DISCUSSION

What insights can be gained from the results above? Several theoretical concepts have been introduced so far trying to explain ultrafast all-optical magnetization manipulation.<sup>12,13,20–23</sup> Since from our experimental investigations we cannot verify all the existing models, we will concentrate in the following on those about which we can draw reliable conclusions. Note that even if not all the considered models have been explicitly applied to explain magnetization switching in GdFeCo so far, it is important to verify if their predictions would be compatible with our findings. This allows us to determine whether such models should be extended to explain the observations for GdFeCo or not. In addition to the verification of current models we also underline the important implications of our results, which should be taken into account for further theoretical investigations and which may finally help to determine the microscopic origin of all-optical switching in GdFeCo.

(a) First, the data presented in Fig. 2 allow us to discuss the applicability of the phenomenological model for all-optical magnetization reversal, which was recently published by Vahaplar and co-workers.<sup>2</sup> In this model a macrospin approach based on the Landau-Lifshitz-Bloch equation was used to describe all-optical switching. To achieve switching it is assumed that the magnetization dynamics is driven by an effective magnetic field  $H_{\text{eff}}$  with time duration  $\Delta t_{\text{eff}}$  induced by the circularly polarized light. Another critical model parameter is the maximal electronic temperature  $T_{\text{el}}^*$  induced by laser excitation. By fixing the value of  $H_{\text{eff}} = 20$  T, the authors calculated a *phase diagram* for all-optical reversal, showing for which combinations of the parameters  $\Delta t_{\text{eff}}$  and  $T_{\text{el}}^*$  all-optical switching can be achieved.

Figure 4 compares the calculated phase diagram [Fig. 4(a)] to a similar diagram extracted from our measurements [Fig. 4(b)]. In order to obtain the diagram in Fig. 4(b), we evaluated the pulse-width-dependent data of the threshold fluence  $F_{\min}$  from the compressor measurements with nearly constant pulse duration steps. This data set, as well as a comparison with the shaper data from Fig. 2, showing identical behavior, can be found in the Supplemental Material.<sup>19</sup> To compare our data set with Fig. 4(a), we evaluated the value



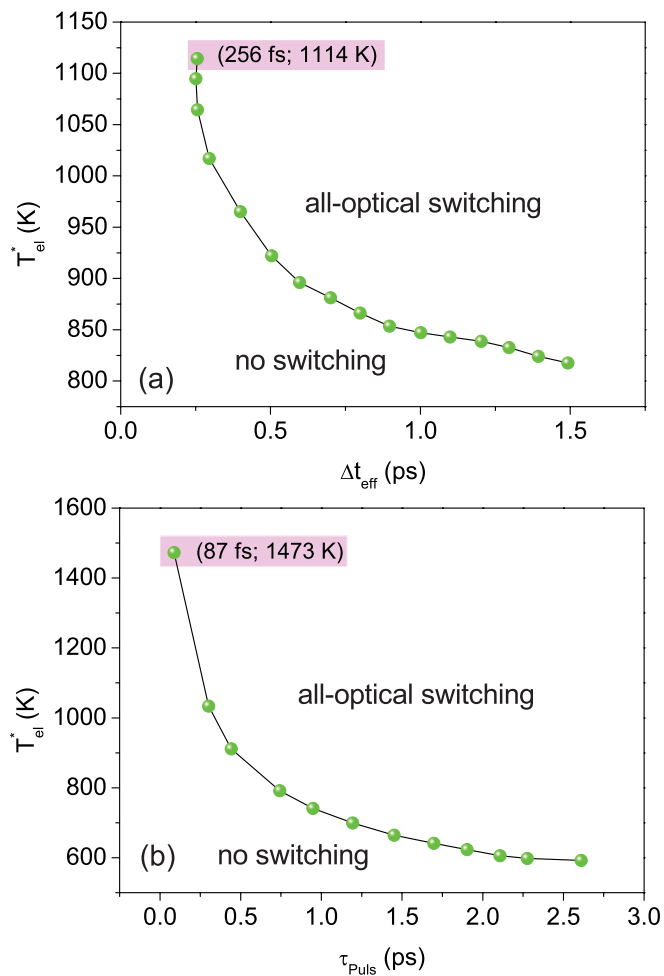


FIG. 4. (Color online) Phase diagrams for all-optical magnetization reversal. (a) Results of the theoretical model of Vahaplar and co-workers, adapted from Ref. 2. The phase diagram shows for which combinations of the parameters  $\Delta t_{eff}$  and  $T_{el}^*$  all-optical switching can be achieved (lower boundary), assuming an effective magnetic field of  $H_{eff} = 20$  T. (b) Phase diagram extracted from our measurements. The laser pulse duration  $\tau_{pulse}$  is extracted from the autocorrelation traces, while the peak electron temperature  $T_{el}^*$  is calculated from two-temperature model simulations assuming 40% absorption, together with experimental laser fluences and durations.

of  $T_{el}^*$  induced by the optical excitation. This was done by using the same material parameters as in Ref. 2 and computing  $T_{el}^*$  with the 2TM. The phase diagram, showing for which combinations of parameters  $T_{el}^*$  and pulse width  $\tau_{pulse}$  we could obtain a switching event in our experiments, is shown in Fig. 4(b).

A first comparison between Figs. 4(a) and 4(b) indicates a rather good qualitative agreement between the two phase diagrams. However, we note that the  $x$  axis in Fig. 4(a) is the effective magnetic-field duration  $\Delta t_{eff}$ , while in Fig. 4(b) it is the laser pulse duration  $\tau_{pulse}$ . So far, the connection between these two quantities is still unknown. First estimates reported in Ref. 2 showed that  $\Delta t_{eff} \gg \tau_{pulse}$ . This is consistent with the fact that in our experiments switching was observed for pulses with  $\tau_{pulse} < 90$  fs, while the minimum value allowed in the theory for  $\Delta t_{eff}$  is 250 fs.

Before we will discuss in more detail what further conclusions can be drawn from the qualitative agreement of the two phase diagrams [see point (f)], let us proceed with discussing what implications concerning the microscopic origin of  $H_{eff}$  follow from our measurements.

The crucial question is what is the microscopic origin of the effective magnetic field? In other words, since the final state of the switching process is determined by the light helicity, where is the helicity information stored after the duration of the laser pulse? In this context, we recall that the electron-hole pairs generated by laser excitation dephase in the material within a few fs only.<sup>11</sup> The helicity information must be transferred from the light field to the system within this time, as the coherence (and therefore the information about the helicity of light) is lost afterwards. As a consequence, the subsystem where the helicity information is stored (the *helicity reservoir*) must be long-lived to allow a significant difference between laser pulse duration and magnetic field pulse duration. However, according to Ref. 1 one does not observe narrow lines in the optical spectrum of  $Gd_{22}Fe_{74.6}Co_{3.4}$ , which would be pointing to the presence of long-lived states. It seems unlikely that such long-lived states exist for the slightly different sample compositions used here, making such a reservoir unlikely. The presence of such a long-living *helicity reservoir* where helicity is stored in the form of angular momentum that can be phenomenologically described as an effective magnetic field  $H_{eff}$  could explain why the intensity for switching only weakly scales with pulse duration in our measurements, as the pulse duration would be of minor importance then.

(b) As a second point we discuss the dependency of  $F_{min}$  on the pulse duration, Fig. 2. No significant variation of  $F_{min}$  is observed despite the pulse length variation of three orders of magnitude (from 45 fs to 10 ps). In Fig. 5 we compare the time evolution of the electron and lattice temperatures after excitation by laser pulses with duration  $\tau = 100$  fs (top panel) and  $\tau = 10$  ps (bottom panel), respectively. The curves have been calculated with the standard two-temperature model (2TM),<sup>18</sup> assuming for both cases a fluence of  $6.22$  mJ/cm<sup>2</sup> and an absorption of 40%. Details on the calculations can be found in Sec. II C. The striking (but well-known) difference between the two cases is that the shorter pulse ( $\tau = 100$  fs) induces an extreme nonequilibrium between the electronic and the phonon system within the first picosecond after excitation. Here, the electronic temperature reaches values above 1000 K, while the phonon system heats up much slower. On a later time scale, the electronic and phonon temperatures eventually equilibrate. On the contrary, for the longer pulse ( $\tau = 10$  ps) the temperatures of the two heat baths are comparable at all time scales. Since for both situations switching is obtained with the same laser fluence, we can conclude that a strong nonequilibrium between the electronic system and the lattice is not necessary to achieve all-optical switching. In other words, we can state that a pronounced peak of the electron temperature does not represent the stimulus of the observed ultrafast reversal, contrary to what is inferred by Ref. 1. In consequence, the peak in the electronic temperature should also not be required to induce the effective magnetic field  $H_{eff}$ .

(c) We now discuss the dependency of  $F_{min}$  on spectral width and chirp, Fig. 2. The broad spectral width of femtosecond laser pulses has been used in the context of

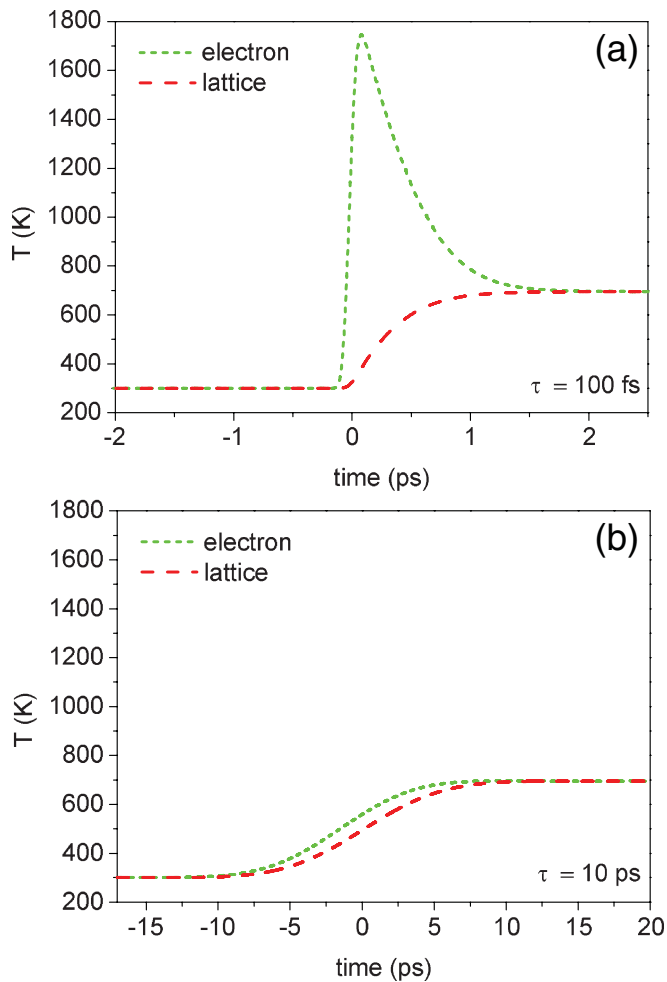


FIG. 5. (Color online) Calculations of the time evolution of electronic and lattice temperatures after excitation with two laser pulses with different time duration  $\tau_{\text{pulse}}$ . The calculations have been performed with the two-temperature model assuming two pulses with  $\tau_{\text{pulse}} = 100$  fs and  $\tau_{\text{pulse}} = 10$  ps, respectively. For both pulses we assumed the same laser fluence of  $6.22$  mJ/cm<sup>2</sup> and absorption coefficient of 40%. The Gaussian laser pulses are centered at time zero. Green short dashed lines indicate the electronic temperature, red long dashed lines indicate the lattice temperature.

the so-called *spin-flip stimulated Raman scattering* (SF-SRS) model (cf., for example, Ref. 13) to describe the interaction of circularly polarized ultrashort pulses with several magnetic systems. For example, a ferrimagnetic garnet film ( $\text{Lu}_{3-x-y}\text{Y}_x\text{Bi}_y\text{Fe}_{5-z}\text{Ga}_z\text{O}_{12}$ ), an antiferromagnetic  $\text{FeBO}_3$  film, as well as a paramagnetic  $\text{Dy}_3\text{Al}_5\text{O}_{12}$  were investigated.<sup>7,8,10</sup> In all cases the observed Faraday signal showed oscillations of the magnetization on the nanosecond or picosecond time scale after excitation, whereby the phase of these oscillations was helicity dependent. This behavior could successfully be explained for all three different materials on the basis of SRS.

Figure 6 gives a schematic representation of SF-SRS. One starts with one electron in the ground state with energy  $E_1$ . The system is transiently polarized by the photon with frequency  $\omega_1$  from the exciting femtosecond laser pulse. The second frequency component  $\omega_2$  induces a spin flip via the

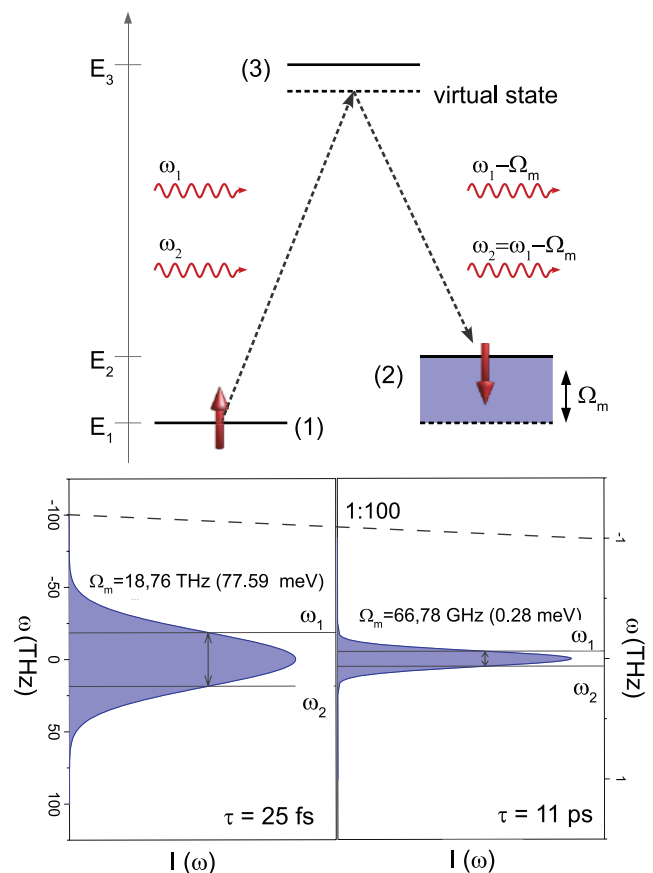


FIG. 6. (Color online) Conceptual principle of spin-flip stimulated Raman scattering (SF-SRS). The frequency component  $\omega_1$  drives a transition from the initial state  $E_1$  into a virtual state. Via stimulated emission due to the presence of the frequency  $\omega_2$  in the pulse spectrum a spin-flip transition to the final state  $E_2$  happens, and a magnon with frequency  $\Omega_m$  is created. The maximal energy difference  $E_1 - E_2$  depends on the spectral width of the laser pulse. For example, a Fourier-transform-limited pulse with 25 fs duration has a bandwidth of 78 meV, while the bandwidth of an 11-ps pulse is only 0.28 meV.

stimulated Raman transition into the state  $E_2$  with  $E_2 > E_1$ . The difference in energy is used to create a magnon with frequency  $\Omega_m$  and a photon with frequency  $\omega_1 - \Omega_m$  is emitted.

The question is now if this model, which was successfully used as a microscopic description of the IFE in dielectrics, may also be applicable to explain all-optical switching in  $\text{GdFeCo}$  as speculated in Ref. 1. In this case, the states  $E_1$  and  $E_2$  represent the equilibrium states of the sample with opposite magnetization direction. As a consequence, the energy difference  $E_1 - E_2$  should be related either to the spin-orbit coupling, whose strength is typically a few tens of meV (in  $3d$  ferromagnets), or to the exchange interaction, with energy scale of hundreds of meV to some eV. Figure 6(a) makes clear that by changing the pulse width from 25 fs to 11 ps, the bandwidth of the laser shrinks from approximately 78 to 0.28 meV. Thus according to our measurements  $E_1 - E_2 \leq 0.28$  meV. This difference is two and three orders of magnitudes smaller than typical values of spin orbit and

exchange interaction, respectively. Altogether we conclude that it is doubtful that a SF-SRS process could induce a measurable change in the magnetization of the sample, although one could theoretically imagine this to happen if the exchange splitting is nearly collapsed near the Curie temperature. This also implies that the exchange splitting would have to collapse on the order of the pulse duration of only a few tens of fs for the shortest pulses, as SF-SRS can only happen during the presence of the laser pulse due to the zero lifetime of the excited virtual state (cf. also Ref. 1). However, we also would like to point out that a nearly total collapse of the exchange splitting is in contradiction with the idea of a nonthermal process.

Another important observation is that, based on the SF-SRS picture, a qualitatively different behavior would be expected for up- and down-chirped pulses. Contrary to this expectation our results are symmetric in the sign of the chirp. This observation can be understood if one takes into account the fact that already a very small bandwidth of 0.063 nm is sufficient to switch all optically. As a consequence, to see a chirp-dependent effect one would have to chirp the pulse so strongly that two frequency components only separated by 0.063 nm are temporally delayed. This is even for our highest GVD values not at all reached and therefore it is clear why no effect of the pulse chirp could be observed, even if SF-SRS would be the correct description. Summarizing, we conclude that spin-flip stimulated Raman scattering is unlikely to be the origin of  $H_{\text{eff}}$ .

(d) The last conclusion that can be drawn from the data of Fig. 2 is that no nonlinear light-matter interaction can be responsible for all-optical switching. In fact, any nonlinear effect depending on the intensity should show a strong dependence of switching threshold with the pulse duration, as peak powers decrease tremendously with pulse lengthening. This is contradictory to the small change in switching threshold observed for all pulse durations (with and without chirp). This implies that the generation of  $H_{\text{eff}}$  should not be based on nonlinear effects.

(e) Finally we discuss the dependency of  $F_{\text{min}}$  on the central wavelength of the laser pulse, Fig. 3, allowing us to draw conclusions about the applicability of the IFE as a microscopic origin for  $H_{\text{eff}}$ . The frequency dependence of the IFE has been investigated theoretically by Hertel,<sup>12</sup> who used a microscopic approach to model the IFE in a transparent metallic medium exposed to a circularly polarized electromagnetic wave. The magnetization  $M$  generated by the light in the medium is predicted to show the dependence  $M \propto \frac{I}{\omega^3}$  on the laser frequency  $\omega$  and intensity  $I$ . Correspondingly,  $F_{\text{min}}$  should show a  $\omega^3$  dependency. This curve is plotted with a solid line in Fig. 3 together with the experimental data. Even being aware that it was difficult to compute the threshold fluence for the data points at  $\lambda = 650, 590, \text{ and } 530 \text{ nm}$ , we come to the conclusion that the difference of a factor of 8 in  $F_{\text{min}}$  between theory and experiment for the data point at  $\lambda = 389 \text{ nm}$  (that can be directly compared to the data at  $\lambda = 777 \text{ nm}$ ) can safely be used to determine that all-optical switching is not compatible with the microscopic approach mentioned above, raising as well some doubts about the IFE as the origin for  $H_{\text{eff}}$  in our system.

(f) Closing, we get back to the question of what further phenomenological information about  $H_{\text{eff}}$  can be obtained

from the agreement of the two phase diagrams discussed in (a). In the suggested model of linear reversal<sup>2</sup> it is (i) necessary that  $T_{el}^*$  reaches the vicinity of  $T_C$  simultaneously with the presence of the effective magnetic field pulse to allow for a reversed magnetization. Furthermore, (ii) if the sample stays above  $T_C$  too long the reversed magnetization is destroyed again.<sup>2</sup> We can use these two statements in combination with our experimental findings to learn about the properties of the induced magnetic field  $H_{\text{eff}}$ .

The first statement (i) tells us that the magnetic field pulse will not evolve faster than the light pulse.  $T_{el}^*$  always follows the evolution of the light pulse, therefore as  $H_{\text{eff}}$  either originates from the light pulse directly or is connected to the electronic system (respectively  $T_{el}^*$ ) it can only be as fast or slower. The phase diagrams of Fig. 4 (as well as Ref. 2) already indicate that  $H_{\text{eff}}$  evolves slower, as the shortest possible magnetic pulse duration for switching is longer than the shortest light pulse duration. The second statement (ii) tells us that the magnetic-field pulse will also persist longer than the light pulse. For our longest pulses [Fig. 5(b)] the electronic system reaches its maximum temperature after the light pulse interaction with the sample is nearly over and stays near that value for longer times. This value must be the value near  $T_C$  [cf. statement (i)], therefore  $H_{\text{eff}}$  has to persist long enough that  $T_{el}^*$  has cooled down sufficiently, else the magnetization is destroyed again [cf. statement (ii)]. Taking the above considerations into account it might be a first idea to model the shape and evolution of  $H_{\text{eff}}$  similar to the shape and evolution of  $T_{el}^*$  after excitation with the laser pulses.

To sum up: Applying the knowledge about the model of Vahaplar and co-workers to our data in Fig. 4(b), we predict that the magnetic-field pulse duration will be generally longer than the laser pulse duration and might be connected to  $T_{el}^*$ . By means of our phase diagram [Fig. 4(b)] it should be possible to extend the simulations by Vahaplar and co-workers to verify these relations between magnetic-field pulses and laser pulses.

As evident from above, the phase diagrams in Fig. 4 suggest the relevance of the parameter  $T_{el}^*$  for all-optical switching. However, we already discussed that a pronounced peak of the electron temperature is not required to stimulate ultrafast reversal. It might be worthwhile to calculate the analogous phase diagram dependent on the lattice temperature  $T_l$ , to gain further insight if  $T_l$  is the relevant parameter for switching.

## V. CONCLUSION

In summary, we investigated the dependence of the lower all-optical switching threshold on pulse duration, chirp, bandwidth, and wavelength for Gd<sub>26</sub>. We found that switching is possible over a large range of pulse durations up to 13 ps using femtosecond and picosecond laser sources with vastly differing spectral bandwidths as well as for different wavelengths of the visible spectra. In addition, we demonstrated that the switching threshold increases only slightly for longer chirped pulses. These are exciting results for technological application, as all-optical switching has been demonstrated for true picosecond laser sources and no pronounced dependence on wavelengths has been observed.

We compared our results to the predictions of the phenomenological model by Vahaplar *et al.*<sup>2</sup> We found a

qualitative agreement of the calculated and measured phase diagram and conclude that a phenomenological description in terms of an effective magnetic field seems to be suitable for all-optical switching. Nevertheless, on the basis of our experimental results the microscopic origin of this field—a still undefined helicity reservoir—must be carefully readdressed. Therefore we used our results to verify some possible mechanisms. In addition we drew some further conclusions about the microscopic properties of all-optical switching: First, we found that no strong nonequilibrium between the electronic system and the lattice is needed to achieve switching. Second, spin-flip stimulated Raman scattering seems unlikely as a mechanism for full magnetization reversal, as the typical energy scales of spin orbit and exchange interactions do not fit the small available bandwidth of picosecond laser pulses. Third, a nonlinear mechanism could be ruled out as well, because the switching threshold is nearly independent from the pulse peak intensity showing that the switching only depends on the number of photons. Moreover, on a microscopic basis the inverse Faraday effect does not correctly describe the switching behavior, as the switching threshold fluence does not show the expected  $\omega^3$  dependence. Furthermore, a resonant process is unlikely, because no strong dependence on wavelength

could be observed. Finally, we also showed that the issue of a helicity reservoir should be carefully addressed. It is our hope that all these results will stimulate further theoretical investigations to reveal the microscopic origin of all-optical switching.

#### ACKNOWLEDGMENTS

We wish to thank the German Science Foundation for funding within the GRK 792 and the European Union for funding within the European Community's Seventh Framework Programme (FP7/2007-2013) under Grant No. NMP3-SL-2008-214469 (UltraMagnetron). The authors thank A. Tsukamoto and A. Itoh (Nihon University) for providing the samples as well as K. Vahaplar, A. Kalashnikova, A. V. Kimel, A. Kirilyuk, Th. Rasing (all RU Nijmegen), K. Bergmann, and M. Fleischhauer (TU Kaiserslautern) for helpful discussion. We thank R. Diller, M. Colindres, and K. Chevalier (TU Kaiserslautern) for valuable support for measurements with their NOPA. Last, we want to thank the Photonik-Zentrum Kaiserslautern e.V., especially J. L'huillier for access to the picosecond laser system and T. Herrmann and M. Stolze for technical support with it.

\*steil@physik.uni-kl.de

†cinchett@rhrk.uni-kl.de

<sup>1</sup>C. D. Stanciu, F. Hansteen, A. V. Kimel, A. Kirilyuk, A. Tsukamoto, A. Itoh, and T. Rasing, *Phys. Rev. Lett.* **99**, 047601 (2007).

<sup>2</sup>K. Vahaplar, A. M. Kalashnikova, A. V. Kimel, D. Hinzke, U. Nowak, R. Chantrell, A. Tsukamoto, A. Itoh, A. Kirilyuk, and T. Rasing, *Phys. Rev. Lett.* **103**, 117201 (2009).

<sup>3</sup>I. Tudosa, C. Stamm, A. B. Kashuba, F. King, H. C. Siegmann, J. Stohr, G. Ju, B. Lu, and D. Weller, *Nature (London)* **428**, 831 (2004).

<sup>4</sup>J. P. van der Ziel, P. S. Pershan, and L. D. Malmstrom, *Phys. Rev. Lett.* **15**, 190 (1965).

<sup>5</sup>A. V. Kimel, A. Kirilyuk, P. A. Usachev, R. V. Pisarev, A. M. Balbashov, and T. Rasing, *Nature (London)* **435**, 655 (2005).

<sup>6</sup>A. V. Kimel, C. D. Stanciu, P. A. Usachev, R. V. Pisarev, V. N. Gridnev, A. Kirilyuk, and T. Rasing, *Phys. Rev. B* **74**, 060403 (2006).

<sup>7</sup>F. Hansteen, A. Kimel, A. Kirilyuk, and T. Rasing, *Phys. Rev. B* **73**, 014421 (2006).

<sup>8</sup>A. M. Kalashnikova, A. V. Kimel, R. V. Pisarev, V. N. Gridnev, A. Kirilyuk, and T. Rasing, *Phys. Rev. Lett.* **99**, 167205 (2007).

<sup>9</sup>V. N. Gridnev, *Phys. Rev. B* **77**, 094426 (2008).

<sup>10</sup>A. H. M. Reid, A. V. Kimel, A. Kirilyuk, J. F. Gregg, and T. Rasing, *Phys. Rev. B* **81**, 104404 (2010).

<sup>11</sup>H. Petek and S. Ogawa, *Prog. Surf. Sci.* **56**, 239 (1997).

<sup>12</sup>R. Hertel, *J. Magn. Magn. Mater.* **303**, L1 (2006).

<sup>13</sup>A. Kimel, A. Kirilyuk, and T. Rasing, *Laser Photonics Rev.* **1**, 275 (2007).

<sup>14</sup>A. M. Weiner, *Rev. Sci. Instrum.* **71**, 1929 (2000).

<sup>15</sup>S. Backus, C. G. D. III, M. M. Murnane, and H. C. Kapteyn, *Rev. Sci. Instrum.* **69**, 1207 (1998).

<sup>16</sup>J.-C. Diels and W. Rudolph, *Ultrashort Laser Pulse Phenomena: Fundamentals, Techniques, and Applications on a Femtosecond Time Scale*, edited by P. F. Liao, P. L. Kelley, and I. Kaminow, *Optics and Photonics* (Academic Press, Boston, 1995).

<sup>17</sup>Note that the compressor itself introduces only negative chirp, but the pulses are very strongly positively chirped before due to the process of chirped pulse amplification.

<sup>18</sup>S. I. Anisimov, B. L. Kapeliovich, and T. L. Perel'man, *Sov. Phys. JETP* **39**, 375 (1974).

<sup>19</sup>See Supplemental Material at <http://link.aps.org/supplemental/10.1103/PhysRevB.84.224408> for details of the compressor-based threshold fluence measurements, as well as spectra of the NOPA-pulses.

<sup>20</sup>S. R. Woodford, *Phys. Rev. B* **79**, 212412 (2009).

<sup>21</sup>M. I. Kurkin, N. B. Bakulina, and R. V. Pisarev, *Phys. Rev. B* **78**, 134430 (2008).

<sup>22</sup>A. Rebei and J. Hohlfield, *Phys. Lett. A* **372**, 1915 (2008).

<sup>23</sup>J. Hohlfield, C. D. Stanciu, and A. Rebei, *Appl. Phys. Lett.* **94**, 152504 (2009).